Self-diffusion along step-bottoms on Pt(111)

Peter J. Feibelman

Sandia National Laboratories

Albuquerque, NM 87185-1413

First-principles total energies of periodic vicinals are used to estimate barriers for Pt-adatom diffusion along straight and kinked steps on Pt(111), and around a corner where straight steps intersect. In all cases studied, hopping diffusion has a lower barrier than concerted substitution. In conflict with simulations of dendritic Pt island formation on Pt(111), hopping from a corner site to a step whose riser is a (111)-microfacet is predicted to be more facile than to one whose riser is a (100).

I) Introduction -

By allowing us to follow at the atomic level how the outer layer of a sample evolves in time, e.g., during epitaxy, high-resolution microscopy offers a glimpse of the energy landscape in which surface atoms migrate. The idea that controlling surface evolution requires learning what conditions make certain mass-transport processes facile and others slow underlines the importance of the clues that scanning probes thereby afford.

Deriving hard knowledge from a sequence of micrographs is, however, a challenging task. Matter-transport on the complicated landscape of an imperfect surface involves many different energy barriers. Thus, it is generally unclear that one's ability to simulate micrographs using a limited set of semi-empirical barriers -- and

DISCLAIMER

DISCLAIMER

Portions of this document may be illegible in electronic image products. Images are produced from the best available original document.

until recently this was the *only* way to derive knowledge from scanning-probe data -- warrants the inference that barriers "that work" correspond to nature in an obvious way.

An additional worry, when *reactive* surfaces are under study, is that data from apparently well-characterized samples may be governed by contaminant effects.[1] The reason is that gas species from the ambient tend to adsorb at defects, such as island edges, where their effects are likely to be particularly large. When this is the case,[1] it is unclear what inferences to draw from agreement of simulations with experiment.[2,3]

Studies by Stumpf and Scheffler,[4] by myself[5] and by Bogicevic, et al.[6] point a way out of the problem. Density Functional methods[7,8] can now be routinely applied to periodic systems with unit cells encompassing tens to hundreds of atoms. Thus, to the accuracy inherent in Density Functional Theory (DFT),[7-10] using periodic model "defective" surfaces, one can compute energetic barriers to surface atom displacement near steps, kinks and vacancies, and *predict* surface morphological changes instead of fitting to them. In complicated cases, where Monte Carlo simulation based on a limited set of barriers is unavoidable, DFT results can be used to constrain the choice of barriers.

Ref. 5, on downward self-diffusion at steps on Pt(111), illustrates how educational DFT results can be. The small (20 meV) reflection barrier calculated there for a Pt atom at a (100)-microfacet step, an "A-type" step in the standard jargon, is inconsistent with the observations[11] that triangular pyramids bounded by A-type steps grow on the clean surface up to ~450K, and that O pre-coverage restores layer-by-layer epitaxy by *reducing* the A-step reflection barrier.

The worrisome inability of DFT to account for these observations had a surprising denouement, when Kalff, et al. reported, independently, that the surface morphologies of Ref. 11 had been strongly affected by adsorption of CO from the vacuum system ambient.[1] *Consistent with DFT energetics*, the Pt islands that grow in the absence of step-bound CO are bounded by (111)- rather than (100)-microfaceted steps.[1,12]

Among the conclusions one may draw from this surprise is that modern DFT calculations are sufficiently realistic and reliable that they can *and should* be used to critique experiment. Though DFT's systematic error level remains a quantitative question,[7] the day is past when one could dismiss the possibility out-of-hand that a gross disagreement between experiment and 1st-principles theory might reflect a systematic *experimental* problem.

In what follows, therefore, I extend consideration of the energy landscape experienced by Pt atoms near steps on Pt(111) to edge-running and corner-rounding barriers. These barriers make the difference between compact, fractal and dendritic[13] islands, and must be part of an effort to simulate the morphology of a growing Pt(111) sample.

For example, Hohage, et al. attribute the occurrence and orientation of dendritic islands on Pt(111) between 150 and 250K to the difference in barriers experienced by a Pt adatom moving from an island corner to an adjacent (100)- or (111)-microfaceted edge.[14] On the basis of simple geometry, they argue that the adatom should move more readily to the (100)-type step, and show via a Monte Carlo simulation that this assumption produces dendritic islands of similar character to those observed experimentally.

Nonetheless, the DFT results reported below predict just the reverse anisotropy, in qualitative agreement with earlier, semi-empirical calculations of Ref. 2 and of Brune, et al.[15] Thus we must explain a disagreement between theory and the apparent implications of experiment, once again.

Making it difficult to ascribe Ref. 14's results to surface contamination, new experiments show that epitaxy under "extremely clean conditions" produces similar dendritic islands, with same orientation.[16] This result underlines the importance of considering ideas such as Brune, et al.'s,[15] that Pt atoms approaching an island might be preferentially guided to (100)-microfaceted edges without ever attaching to the corner. In this scenario, the corner-to-edge barrier anisotropy is irrelevant.

To obtain DFT barriers, I compute total energies of representative periodic Pt vicinal surfaces, with Pt adatoms placed in appropriate locations. Pt(854), for example, has (100)-microfaceted steps (henceforth referred to as "A-type"), interrupted by a kink every fourth atom and separated by (111)-terraces 4 atomic rows wide (see Fig. 1). Pt(874) similarly represents kinked (111)-microfaceted (henceforth "B-type") steps, and a 2x1 "reconstruction" of Pt(432) is convenient for the study of diffusion around the 120° corners where the two types of step meet.

These vicinals involve a substantial number of inequivalent atoms per surface unit cell. That their energies can now be calculated routinely testifies to the enormous power of modern parallel computers and the sophisticated Vienna *Ab Initio* Simulation Package (VASP),[17-19] which I have employed.

The computed barrier energies summarized in Tables 1-3 embody several significant results beyond the barrier anisotropy just discussed:

1) In all cases considered, i.e., for straight and kinked A- and B-type steps and around corners between them, diffusion by concerted substitution (CS), in

which a step-edge atom emerges onto the terrace and is simultaneously replaced by the initial adatom, is considerably less facile than by ordinary adatom hopping. Within the Local Density Approximation (LDA),[10] the CS barriers are 0.3 to 0.4 eV higher than those for hopping.

2) Hopping barrier energies mainly reflect *local* geometry, i.e., the arrangement of the adatom's nearest neighbors along its diffusion path. Thus, hopping from a corner to an adjacent step-edge site costs close to the same energy whether the corner represents a kink, as on Pt(854) or Pt(874), or the intersection of an A- and a B-type step, as on Pt(432).

3) For the same reason, but perhaps more surprisingly, barriers to diffusion along straight steps and around corners are also not very different, ranging between 0.8 and 1.0 eV. This result reflects an "early barrier" for an adatom moving around a corner, experienced as it moves parallel to the step-bottom where it is initially bound.

4) The computed barriers are roughly twice as large as the semi-empirical results of Refs. 2 and 15.

The remainder of this article is organized as follows: In Sec. II, I provide relevant details of the numerical calculations. Sec. III is devoted to presentation and explanation of the resulting diffusion barriers. In Sec. IV I compare to experiment, where possible, and to earlier calculations based on semi-empirical force laws. Finally, in Sec. V I discuss directions for further study.

II) Numerical methods -

The DFT results reported here were obtained using the efficient and accurate total-energy and molecular-dynamics package, VASP (Vienna *ab-initio* simulation

package),[17-19] its corresponding ultrasoft-pseudopotential data-base,[22] and either the local exchange-correlation potential of Ceperley and Alder,[23] or the Perdew-Wang '91 Generalized Gradient Approximation (GGA).[8] Although plane-wave calculations for d-electron metals typically require unwieldy basis sets, use of an ultrasoft pseudopotential assures convergence of total energy differences with modest basis-cutoffs, specifically, 14 Ry for Pt. To accelerate electronic relaxation, I use the Fermi-level smearing approach of Methfessel and Paxton, with a width = 0.2 eV.[24]

As noted above, I estimate diffusion barriers by comparing total energies of periodic vicinal thin slabs whose geometries correspond to the beginning and end of a diffusion step, and the transition, or saddle point between them. I set the slab lattice parameter to the optimal bulk LDA or GGA value, namely 3.91 or 3.99 Å (experiment = 3.92 Å). To locate transition geometries I use Jónsson's "nudged elastic band" (NEB) scheme,[25] typically placing four slab replicas between the initial and final configurations and determining the barrier energy via a spline fit.[26] The barrier energies quoted are numerically accurate to ~20 meV.

The following subsections provide specifics of the vicinal slab calculations that represent diffusion along the bottoms of A) straight steps and B) kinked steps, and C) around the 120° corners where A- and B-type steps intersect.

A) Diffusion along unkinked A- and B-steps - To estimate diffusion barriers for straight A- and B-type steps, I compare total energies of 3x1 arrangements of Pt adatoms on 20-layer Pt(322) and 18-layer Pt(221) slabs (see Figs. 2a and b), in each case fixing the lower five atomic layers in their bulk DFT positions, and relaxing all the rest. The (322) and (211) slabs have rectangular primitive unit cells, whose reflection symmetry is conveniently unaffected by adding 3x1 arrangements of ada-

toms along the step bottoms. Their (111)-terraces are 5 and 4 atomic rows across, sufficiently wide that step-to-step interaction effects are small. The same applies to the separation of the adatoms in the assumed 3x1 adsorption geometry.

I relax electronic densities till the total energy is converged to $\sim5\times10^{-6}$ eV/atom and geometries till the forces on unconstrained atoms are below ~0.03 eV/Å. Because the bonding of Pt is dominated by d-electrons, which occupy relatively flat bands, and aiming for 20 meV accuracy in diffusion barriers, the Surface Brillouin Zone sample I have used, comprised of 16 equally spaced k-vectors, is conservative.

For the sake of a consistency check (see Sec. IIID), I also report step-bottom adsorption energies on a Pt(111)-$3\times4\sqrt3$ supercell slab whose surface is a periodic array of stripes. As Fig. 2c makes plain, the valleys on such a surface are bounded on one side by an A-type step and on the other by a B-step.[4] Thus Pt binding energies at A- and B-type steps can be subtracted with optimal error cancellation. The energies reported below for the stripe-islands correspond to a slab whose stripe-islands and the valleys between them are both four atomic rows across. The slab is five layers thick in the valley regions. The stripes thus represent half a sixth layer. In these calculations I sample the Brillouin zone with 8 equally spaced k's.

B) Diffusion at kinked A- and B-type steps - To study diffusion around kinks, I compute total energies of the Pt(854) and (874) surfaces, which are illustrated in Figs. 1 and 3. Pt(854) is comprised of terraces four atomic rows wide between A-type steps that have a kink every fourth atom (see Figs. 1). Pt(874) also has terraces 4 atom rows across between steps kinked every fourth atom (see Figs. 3). On this crystal plane, however, the kinked steps are B-type.

To limit quantum size effects, I represent the (854) and (874) surfaces of Pt

by 61 and 64 layer slabs whose thicknesses are roughly equal to that of a 5-layer Pt(111) film. In each case I fix the positions of the lower 24 atomic layers at their bulk DFT positions and allow the remainder to relax. Force and energy tolerances are as in the straight-step calculations.

As a check on the convergence of the calculated energies with the size of the surface Brillouin zone sample, I compare Pt(874) results corresponding to 4 and 16 k-vector samples. The results agree to ~20 meV, implying that the 16-k sample gives a sufficiently accurate picture.

C) Diffusion at the intersection of an A- and a B-type step - For diffusion near intersections of A- and B-type steps, I calculate the energetics of hypothetical 2x1 reconstructions of Pt(432), as illustrated in Figs. 4. Displacing atoms "*a*" in the unreconstructed geometry of Fig. 4a to the right, I arrive at the geometry of Fig. 4b, where they are now located on the A-step side of corner site, γ. Moving them farther, or substituting them for corner-atoms "*B*," as in Fig. 4c, I can estimate the energetics of corner rounding by either site-to-site hopping or concerted substitutional diffusion. The results reported correspond to 52 atomic layer 2x1-(432) slabs whose thickness is roughly that of four (111)-layers. The lower eight 2-atom layers are fixed at bulk DFT relative positions and the rest relaxed. Here as in the other cases studied, I use a full SBZ sample of 16 equally spaced k's.

III) Computed diffusion barriers -

In the following subsections I present and discuss the calculated energetics of self-diffusion along the bottoms of A) straight and B) kinked steps on Pt(111) and C) around the 120° corners where A- and B-type steps intersect on the same surface. In subsection D) I show that, to within a reasonable level of accuracy, the results presented are in accord with the principle of detailed balance. Because LDA

hopping barriers are several tenths of an eV lower than CS barriers (cf. Table 1), the discussion focuses on hopping.

A) Diffusion along unkinked A- and B-steps - Calculated and measured edge-running barriers (see Table 2) are roughly two and a half times larger than the self-diffusion barrier on Pt(111), which equals 0.29 eV in both the LDA and the GGA. At first glance this difference may seem surprising, since the number of an adatom's near neighbors diminishes by only one as it displaces along a step bottom to the barrier geometry -- just as on a perfect (111) terrace. A more serious look at bond lengths, however, shows that coordination loss in displacement to the step-bottom barrier geometry is considerably greater than in diffusion on a (111) terrace.

Specifically (see Table 4), on a (111) surface the cost of displacing an adatom from its initial fcc 3-fold hollow to a bridge is that of replacing three longer bonds by two shorter ones (shorter by 2%). In contrast, in the barrier geometries for diffusion along A- and B-type steps, the adatom's initial five bonds are replaced by two short ones and two long ones. At an A-step, after elimination of one bond to a step-edge atom, one other shortens by 4%, one is replaced by bond that is 6% longer and two others remain of roughly the same length. At a B step, beyond eliminating one short bond, displacement to the barrier means shortening two bonds by 7% each, and replacing two others with bonds longer by 8% and 4%. Thus, compared to a (111) terrace, the barrier to displacement along a step bottom is relatively large because the loss of one rather strong bond is poorly compensated, overall, by strengthening of the remainder.[4]

B) Diffusion along kinked steps - Usually, hopping from an edge-site into a kink will take place in two steps (cf. Figs. 1 and 3). First the adatom will move from the edge, where it has five neighbors, to a corner site where, having lost contact with an

upper terrace atom, it has just four. Then, barring a return to the edge, it will displace into the kink where it has six neighbors and is tightly bound.

At a kinked B-step, according to the present calculations, displacement from the 5- to the 4-fold site is only weakly affected by the reduced coordination of the final state. Within the LDA(GGA), the barrier is 0.89(0.74) eV, as against 0.90(0.77)eV for hopping along the straight B-type step. This suggests that the B-edge-to-corner barrier is largely determined locally.[4] In other words, it occurs "early" enough that the absence of a next-nearest step-edge neighbor in the barrier geometry is of little consequence.

The bond-length comparison in Table 5 supports this picture. The shortest adatom bond lengths for B-edge-to-corner diffusion on Pt(874) are within 0.01Å of the corresponding lengths at the barrier for diffusion along the straight B-step of Pt(221). The next-longer bonds, to step-bottom atoms B_1 and B_2 in Fig. 3b, are also relatively close in length, 2.71 and 2.79Å, to the corresponding bond lengths, 2.76 and 2.76Å, in the barrier geometry on Pt(221).

That the adatom's bonds to B_1 and B_2 are of *different* lengths reflects the kink-related asymmetry of the energy landscape near the diffusion barrier. That these lengths are not *very* different means the asymmetry is weak.

In the A-edge-to-corner barrier configuration on Pt(854), the lengths of the two shortest bonds between adatom and its substrate neighbors are also close to what is found for diffusion along the corresponding straight edge (see Table 5) -- and as for the B-step case, the lengths of next longer bonds, $\overline{AT_1}$=2.66Å and $\overline{AT_2}$=2.92Å (see Fig. 1b) bracket the corresponding straight-edge barrier bond lengths, 2.73 and 2.73 Å. However, given that bond strength is quite sensitive to bond length, the 0.26Å difference between $\overline{AT_1}$ and $\overline{AT_2}$ signals a not-so-weak

asymmetry of the near-kink energy landscape, and a significant effect on diffusion.

It is therefore not a surprise that the barrier to displacing from the 5- to the 4-fold site is *not* identical to the diffusion barrier along the straight A-type step, but more than 0.1 eV higher. More precisely, on Pt(854), within the LDA(GGA), the A-edge-site-to-corner barrier is 0.96(0.82) as against 0.84(0.71) eV for hopping along the straight A-type step.

It is important to appreciate that, by the principle of detailed balance, any effect on an edge-to-corner barrier has a corresponding effect on the reverse process, in this case on corner-to-edge displacement. Moreover, locality of bonding implies that the binding energies of adatoms in corner sites on the kinked A- and B-type steps of Pt(854) and (874) must be roughly equal. On the basis of the edge-to-corner barriers just discussed (refer to Table 2 for a summary), one can therefore expect the corner-to-B-edge activation energy on Pt(874) to be about 0.08 eV smaller than the corner-to-A-edge barrier on Pt(854). In agreement with this expectation, the calculated LDA(GGA) corner-to-edge barrier is 0.40(0.37) eV for the kinked B-type step and 0.51(0.46) eV for the kinked A-step.

This corner-to-edge barrier difference is of the order of magnitude needed to explain the formation of dendritic islands in epitaxy on Pt(111),[27] but it has the wrong sign to explain their orientation.[14] Implications of this discrepancy are discussed below. First, however, it is worth trying to gain some understanding of the physics that gives rise to the barrier anisotropy.

To this end, note that while the adatom diffusion path from corner to B-edge site is essentially a straight line parallel to the B-step (cf. Figs. 3), for displacement from corner to an A-edge matters are different. In that case (see Fig. 1a), the atoms on the lower terrace first guide the adatom away from corner atom C and toward

hcp hollow, h, then back toward the first 5-fold coordinated A-edge site. On a straight A-edge, sufficiently far from a kink, the diffusion barrier geometry is symmetrically located between neighboring 5-fold sites, where a "zig" ends and a "zag" begins. But immediately at a kink, the first "zig" coupled with the strong pull of the undercoordinated corner atom produces an asymmetric barrier and a correspondingly higher activation energy for diffusion.

In Ref. 15, Brune et al. remark that *strain relief* is the source of the low corner to B-edge barrier. The idea is that the short bonds required in the B-edge barrier geometry are favored by Pt, whose relatively low temperature reconstructions identify it as a high-surface stress material. The semi-empirical calculational evidence is that on a "low stress" Ag surface, Ag atoms prefer to diffuse from corners to A- rather than B-edges.

Whether these thoughts will be supported by stress-relief calculations remains to be seen. It is clear from the present calculations, though, that the barrier to diffusion from a corner to a B-edge site is virtually identical to that for displacement along a straight B-step. Thus, whatever the contribution of stress relief may be, it is the same near a kink as far from one. This argument casts doubt on the stress-relief explanation of the barrier anisotropy. What is different near a corner as against a straight edge is the asymmetric organization of the atoms on the A-step side of the corner. That, coupled with the low coordination of the corner atom, is the most likely source of the computed high barrier against corner-to-A-edge displacement.

C) Diffusion around intersections of A- and B-type steps - As in edge-to-kink displacement, an adatom will usually hop in two steps around a 120° corner where an A- and a B-type step intersect. First displacing from an edge 5-fold site to

a corner 4-fold geometry, the adatom will then move on to a 5-fold site on the other edge. According to Table 2 the barriers for displacement between 4- and 5-fold sites at a corner on Pt(432) are within 20 meV of the barriers for the corresponding displacements at the bottoms of the kinked steps of Pt(854) and Pt(874), one last consequence of locality.

These results confirm that displacement from a corner site to a B-step edge is *more*, rather than less facile than to an A-step edge site -- specifically, the LDA(GGA) barrier against displacement from a corner-site to the B-type edge is 0.09(0.06) eV smaller than to the A-edge. As was proposed at the end of the previous section, the source of this difference is likely the conflict between the zig-zag diffusion path imposed by the lower terrace, as one moves from corner to A-edge, and the need to coordinate as strongly as possible to the corner atom. In any event, accepting the validity of the numerics, it remains to explain the orientation of the dendritic islands observed in Ref. 14, which according to simulations,[14,15] require that the corner-to-B-edge barrier be the lower.

D) Consistency of the calculated energies - Before comparing calculated to measured edge-running and corner-rounding barriers, it is important to consider the consistency of the calculated results -- and at first glance, there is some reason for concern. Since A-type steps have a higher formation energy than B-type,[29] the former should be more reactive and should bind Pt adatoms more strongly.[4,30] Notwithstanding, the Pt(432) barriers in Table 2 imply[28] a negligible LDA binding energy difference between 5-fold sites immediately on the A- and B-step sides of a corner. In the GGA (see Fig. 5), the difference is also small; the A-step site is favorable by only 0.02 eV.[31]

Why does displacing an atom from the A- to the B-side of a corner incur vir-

tually *no* energy cost? Without responding to this question directly, an obvious reply is that there is no reason that binding energies at 5-fold edge sites adjacent to corners should be the same as at 5-fold sites farther down an edge. In fact, based on FIM observations, Fu, et al.[32] show that just such an energy difference exists for an Ir adatom on the A-step side of an island corner on Ir(111), and amounts to ~0.03 eV.

No comparable result has yet been reported for Pt. In the meantime, however, it is of interest to compute the energy required to displace a Pt adatom from a straight A- to a straight B-edge site, and verify that it is positive and substantial. To this end, I optimize adatom geometries on striped (111)-slabs (cf. Sec. IIA). Within the LDA(GGA), using the supercell schematized in Fig. 2c, I find that a Pt adatom should gain 0.11(0.13) eV in moving from a B- to an A-type step, in qualitative agreement with the idea that the step with the higher formation energy should be more attractive to an adatom.[29]

IV) Theory vs. experiment -

Comparison with available data (cf. Table 3) establishes that the reliability of DFT self-diffusion barrier calculations for Pt(111) and its vicinals is in the neighborhood of 10%. For example, the computed barrier for adatom hopping on Pt(111), is ~0.29 eV in both LDA and GGA, while Field Ion[33,34] and Scanning Tunneling Microscopy[35] (FIM and STM) concur on an experimental value of ~0.26 eV.

Edge-running along the bottom of a B-type step is represented in the literature by Bassett and Webber's FIM measurement of self-diffusion on Pt(331).[19] They obtain a barrier of (0.84±0.10) eV, which is bracketed by LDA and GGA barriers of 0.90 and 0.77 eV.

The only experimental results available for edge-running along an A-type step are for self-diffusion on Pt(311). As Figs. 6 make clear, one can scarcely speak of (111) terraces on this vicinal, since they are only two atomic rows wide. Comparison with edge-running barriers computed for Pt(322), whose (111) terraces are 5 atomic rows across, is therefore not quite fair.

Instead, I have directly computed barriers for diffusion along the grooves of Pt(311) for comparison to experiment. They are 0.77eV (LDA) and 0.64eV (GGA), compared to FIM-based measurements yielding (0.69±0.20) and (0.60±0.03) eV.[20,21] The GGA result is in rather close agreement with experiment, evidently, while the LDA barrier is rather too high.

Before leaving the case of Pt(311), it is worth considering why its grooves impose a smaller barrier to diffusion than that which hinders A-step edge-running on Pt(322). A plausible answer (cf. Figs. 6) is that when an adatom displaces from five-fold to four-fold coordination geometries on Pt(311) it remains coordinated to *three* step-edge atoms. In contrast, at an A-type step-bottom, the adatom moves from an initial site where it has two edge-atom neighbors to a site where it has just one.

Since step-edge atoms are the least well coordinated substrate atoms on a vicinal with straight steps, they are the atoms in greatest need of an additional neighbor. Thus, binding to more edge atoms reduces the system energy, and in particular the relative energy of the barrier geometry on Pt(311), illustrated in Fig. 6b.[36]

Given that DFT produces self-diffusion barriers in reasonably good agreement with experiment for vicinals to Pt(111) with straight steps, there is no reason to expect it to fail for diffusion around kinks and corners. The result that displacement from a corner-site to a B-edge is more facile than to an A-edge must therefore

be taken seriously, and a way must be found to reconcile it with the simulations of dendritic island orientation performed by Hohage, et al. in Ref. 14.

As mentioned above, Brune, et al.,[15] point out that corner-to-edge barriers may be irrelevant to dendritic island morphology, because Pt atoms approaching an island may be preferentially guided to A-type edges without ever attaching at a corner-site. Thus, they argue in essence that because the simulations of Ref. 14 leave out key processes, they yield barriers which contradict theory.

In light of Ref. 1, prudence dictates, before computing more barriers and performing further simulations, that one dispose of the possibility that the experimental corner-rounding preference might appear reversed as a result of step-edge-adsorbed contaminants. That this has been accomplished is the message of Ref. 16, which shows that even with a level of step-contamination by CO much below the already low level of Ref. 14, the dendritic-island orientation is no different.

V) The future -

A host of studies makes it clear that the morphology of virtually any growing surface can be simulated by making "reasonable" assumptions concerning binding and barrier energies and applying the Monte Carlo technique. But such *a posteriori* analysis entails several problems:

1) It is not clear that a set of binding energies and barriers that works provides a uniquely sensible fit to the available data.

2) It is not clear how processes left out of consideration might shift the energies one determines via a fit.

3) If sample characterization is inadequate, it is not clear what system the fit barriers correspond to, and the degree to which they are 'transferable' for analysis of other data.

The fact that we can now perform first-principles calculations for relatively low-symmetry, large unit-cells, containing essentially any atomic species, and the existence of numerous cases where results of such calculations are in reasonably good agreement with experiment, points to a near future in which Monte Carlo simulation will no longer be a fitting technique, and in which DFT results will routinely be used to assess the adequacy of surface characterization.

In the quest to simulate epitaxy on clean Pt(111), several barriers (and all prefactors!) remain to be determined - those for downward transport at a kink, for adatom capture by a step and by a kink, and for diffusion of small clusters. Learning their magnitudes, and thus establishing Pt(111) growth as a predictive test-bed for the theory of epitaxy, is a very appealing goal.

REFERENCES -

1. M. Kalff, G. Comsa, and T. Michely, Phys. Rev. Lett. **81**, 1255(1998).

2. J. Jacobsen, K. W. Jacobsen. P. Stoltze and J. K. Nørskov, Phys. Rev. Lett. **74,** 2295(1995).

3. M. Villarba and H. Jónsson, Surf. Sci. **317**, 15(1994).

4. R. Stumpf and M. Scheffler, Phys. Rev. **B53**, 4958(1996).

5. P. J. Feibelman, Phys. Rev. Lett. **81**, 168(1998).

6. A. Bogicevic, J. Strömquist and B. I. Lundqvist, Phys. Rev. Lett. **81**, 637(1998).

7. *The Theory of the Inhomogeneous Electron Gas*, edited by S. Lundqvist and N. H. March (Plenum Press, New York, 1983); also, W. E. Pickett, Comp. Phys. Rep. **9**, 115(1989).

8. J. P. Perdew, in *Electronic Structure of Solids '91*, edited by P. Ziesche and H. Eschrig (Akademie Verlag, Berlin, 1991); J. P. Perdew and Y. Wang, unpublished.

9. P. Hohenberg and W. Kohn, Phys. Rev. **136**, B864 (1964).

10. W. Kohn and L. J. Sham, Phys. Rev. **140**, A1133 (1965).

11. S. Esch, M. Hohage, T. Michely and G. Comsa, Phys. Rev. Lett. **72,** 518(1994).

12. Kalff, et al. explain that pyramids bounded by (100)-microfaceted steps do not grow above ~450K because at such temperatures CO no longer adsorbs, and that oxygen promotion of Pt(111) layer-by-layer growth below ~450K (cf. Ref. 11) has nothing to do with reflection-barrier reduction -- it occurs because O burns off the ad-CO. CO evaporation also accounts for the T-dependence of island shapes on Pt(111) reported by T. Michely, M. Hohage, M. Bott and G. Comsa, Phys. Rev. Lett. **70,** 3943(1993).

13. "Dendritic" means "branched, but manifesting preferred branch directions."

14. M. Hohage, M. Bott, M. Morgenstern, Z. Zhang, T. Michely, and G. Comsa,

Phys. Rev. Lett. **76**, 2366(1996).

15. H. Brune, H. Röder, K. Bromann, K. Kern, J. Jacobsen, P. Stoltze, K. Jacobsen, and J. K. Nørskov, Surf. Sci. **349**, L115(1996).

16. M. Kalff, G. Comsa and T. Michely, (Jülich-Bericht, 1999, unpublished). Also working *against* significant CO contamination effects is the fact that that there are ~20 times as many edge sites per deposited Pt, and thus a ~20 times lower CO step-coverage when dendritic rather than compact islands form. Low H_2 and H_2O dissociative sticking probabilities should also prevent much H from adsorbing in a short data collection interval. T. Michely (private communication).

17. G. Kresse and J. Hafner, Phys. Rev. **B47**, 558 (1993); *ibid.* **B49**, 14251 (1994).

18. G. Kresse and J. Furthmüller, Comput. Mat. Sci. **6**, 15 (1996).

19. G. Kresse and J. Furthmüller, Phys. Rev. **B54**, 11169 (1996).

20. D. W. Bassett and P. R. Webber, Surf. Sci. **70**, 520(1978).

21. G. L. Kellogg, J. Phys. (Paris) **47**, C2-331(1986).

22. D. Vanderbilt, Phys. Rev. **B41**, 7892(1990); A. Pasquarello, K. Laasonen, R. Car, C. Lee and D. Vanderbilt, Phys. Rev. Lett. **69**, 1982(1992); K. Laasonen, A. Pasquarello, R. Car. C. Lee and D. Vanderbilt, Phys. Rev. **B47**, 10142(1993); G. Kresse and J. Hafner, J. Phys.: Cond. Mat. **6**, 8245(1994).

23. D. M. Ceperley and B. J. Alder, Phys. Rev. Lett. **45**, 566(1980), as parameterized by J. Perdew and A. Zunger, Phys. Rev. **B23**, 5048(1981).

24. M. Methfessel and A. T. Paxton, Phys. Rev. **B40**, 3616(1989).

25. H. Jónsson, G. Mills, K. W. Jacobsen, in *Classical and Quantum Dynamics in Condensed Phase Simulations*, ed. B. J. Berne, G. Ciccotti and D. F. Coker (World Scientific, 1998).

26. Scripts by R. Stumpf (unpublished) make launching VASP computations and

analyzing the results particularly easy.

27. H. Jónsson, private communication.

28. As is easy to see in Fig. 5a, the corner to A-side barrier minus that for the reverse process equals the A-side binding energy relative to that at the corner. The B-side vs. corner binding energy difference is obtained analogously. Comparing these differences yields the relative binding energy in the A- and B-side sites.

29. T. Michely and G. Comsa, Surf. Sci. **256**, 217(1991); G. Boisvert, L. J. Lewis and Matthias Scheffler, Phys. Rev. **B57**, 1881(1998).

30. R. C. Nelson, T. L. Einstein, S. Khare and P. J. Rous, Surf. Sci. **295**, 462(1993).

31. This result cannot simply be checked by comparison to the calculated energetics of adatoms on Pt(854) and Pt(874). The reason is that such a comparison, given that there is only one corner site on Pt(432)-2x1, requires the corner-site adatom binding energies in the two kinked-step calculations to be the same. That removing an atom from a kink in an A- or a B-type step costs the same energy on a semi-infinite substrate, and that bonding energetics is approximately local, together suggest that calculated corner-site energies on Pt(854) and Pt(874) should be close, but not necessarily close enough to allow a meaningful check on the relative binding energies computed for Pt(432).

32. T. Y. Fu, Y. R. Tzeng and T. T. Tsong, Surf. Sci. Lett. **366**, L691(1996), Phys. Rev. **B54**, 5932(1996).

33. P. J. Feibelman, J. S. Nelson and G. L. Kellogg, Phys. Rev. **B49**, 10548(1994).

34. K. Kyuno, A. Gölzhäuser and G. Ehrlich, Surf. Sci. **397**, 191(1998).

35. M. Bott, M. Hohage, M. Morgenstern, T. Michely and G. Comsa, Phys. Rev. Lett. **76**, 1304(1996).

36. Pursuing this argument, one expects hopping in the [$\bar{1}$10]-direction on a (110)

surface to face a higher barrier than on other vicinals with B-type steps, e.g., the (331) surface. The reason is that on the (110) surface the adatom loses *two* edge neighbors as it moves to the barrier, as against just one on the (331). It remains to be understood why this "rule" is *not* followed in self-diffusion on Rh(110) and (331), as studied by G. Ayrault and G. Ehrlich, J. Chem. Phys. **60**, 281(1974), nor for Pt on Pt(110) and (331), as reported in Ref. 20, nor for Ni on its (110) and (331) surfaces, as measured by R. T. Tung and W. R. Graham, Surf. Sci. **97**, 73(1980). This question notwithstanding, the diffusion barriers reported for transition-metal (311) surfaces *are* universally smaller than for their (331) faces. See, Ayrault and Ehrlich, *op. cit*, for Rh, Ref. 32 for Ir, Ref. 20 for Pt and Tung and Graham, *op. cit.*, for Ni.

Figure Captions -

1. Ball model of the periodic vicinal, Pt(854), whose A-steps have a kink every fourth atom. Panel a): the adatom, A, is shown in a 4-fold coordination site, in each unit cell, adjacent to a kink. From there it may displace into the 6-fold kink site β, or it may zig-zag onto the A-edge through hcp and fcc hollows, h and f . Panel b): The adatom is in the transition barrier geometry between the step-edge and corner sites. Its bonds to terrace atom T_2 and T_1 differ by 0.26 Å in the LDA, the former being shorter.

2. An adatom, A, bound in a 5-fold coordinated step-bottom site on a) Pt(322), b) Pt(221) and c) on the A-step side of a valley between two monolayer-high stripe islands on Pt(111). Panels a) and b) represent the vicinals used to compute diffusion barriers along unkinked A- and B-type steps. Panel c) shows the surface used to establish a common energy zero.

3. Ball model of the periodic vicinal Pt(874), whose B-type steps have a kink every fourth atom. Panel a) Adatom, A, is shown in a 4-fold corner site, in each unit cell, from which it might move to the 5-fold edge site on its right, γ, or the 6-fold coordinated kink site, β, on its left. Panel b): The adatom is in the transition barrier geometry between the step-edge and corner sites. Its bonds to step-bottom atoms B_1 and B_2 differ by only by 0.08 Å in the LDA.

4. Illustrations showing how the periodic vicinal, Pt(432), is used to estimate corner-rounding barriers. 2x1 reconstructed geometries are relaxed, in which the atoms labeled A in panel a) are moved either of 5-fold edge sites, α or β, or to 4-fold corner site, γ. Minimum energy paths between these sites are then computed using Jónsson's NEB method (Ref. 25). Panel b) shows atoms A in the edge site on the A-type side of γ. Panel c) illustrates the transition geometry for a concerted substitution in

which corner atom B emerges onto the lower terrace and is simultaneously replaced by atom A.

5. Corner-rounding energetics on Pt(432) from the GGA column of Table 2. Note (see dashed line) that binding on the A- and B-sides of the corner is close to equally strong.

6. Schematic of a periodically repeated adatom on Pt(311). Panel a) shows the adatom in its optimal 5-fold coordination site. Panel b) shows it in the 4-fold barrier geometry. In both cases the adatom has three edge neighbors (defined as atoms that are seven-fold coordinated when the adatom is absent).

Table Caption -

1. Comparison of LDA hopping and concerted substitution barriers (in eV) for self-diffusion on various vicinals to Pt(111).

2. Comparison of hopping self-diffusion barriers (in eV) for various surfaces vicinal to Pt(111), calculated within the LDA and the Generalized Gradient Approximation (GGA).[8]

3. Comparison of 1st-principles LDA and GGA, semi-empirical and experimental edge-running and corner-rounding barriers (in eV).

4. For adatom diffusion along the bottom of an A-type and a B-type step, and on a step-free Pt(111) plane, lengths of the adatom's shortest bonds -- in its lowest energy, high coordination site, and in the diffusion barrier geometry. The letters in parenthesis indicate the identity of the substrate neighbor for each bond. Thus "e" indicates a bond to a step-edge neighbor, "b" to a step-bottom neighbor and "t" to a terrace neighbor. The numbers given correspond to LDA calculations for Pt/Pt(322), Pt/Pt(221) and Pt/Pt(111).

5. Comparison of bond lengths in barrier geometries corresponding to diffusion along straight steps and from edge to corner sites on kinked steps. The letters in parenthesis indicate the identity of the substrate neighbor for each bond. Thus "e" indicates a bond to a step-edge neighbor, "b" to a step-bottom neighbor and "t" to a terrace neighbor. The numbers given correspond to LDA calculations for Pt/Pt(322), Pt/Pt(854), Pt/Pt(221) and Pt/Pt(874).

Table 1:

Vicinal	Step type	From	To	Fig.	E_{hop}	E_{CS}
Pt(322)	A	5-fold	5-fold	2a	0.84	1.34
Pt(221)	B	5-fold	5-fold	2b	0.90[a]	1.55
Pt(854)	kinked A	5-fold	6-fold	1	0.96	1.34
Pt(874)	kinked B	5-fold	6-fold	3	0.89	1.30
Pt(432)	120° corner	A-side	B-side	4	0.99	1.44
Pt(432)	120° corner	B-side	A-side	4	0.90	1.45

[a]This compares to an FIM value (see Ref. 20) of 0.84±0.10 eV at B-steps on Pt(331).

Table 2:

Vicinal	Step type	From	To	Fig.	LDA[a] $E_a(eV)$	GGA[b] $E_a(eV)$
Pt(322)	A	5-fold	5-fold	2a	0.84	0.71
Pt(221)	B	5-fold	5-fold	2b	0.90[c]	0.77[c]
Pt(854)	kinked A	5-fold	4-fold	1	0.96	0.82
Pt(854)	kinked A	4-fold	6-fold	1	0.45	0.42
Pt(854)	kinked A	6-fold	4-fold	1	1.32	1.08
Pt(854)	kinked A	4-fold	5-fold	1	0.51	0.46
Pt(874)	kinked B	5-fold	4-fold	3	0.89	0.74
Pt(874)	kinked B	4-fold	6-fold	3	0.39	0.35
Pt(874)	kinked B	6-fold	4-fold	3	1.39	1.13
Pt(874)	kinked B	4-fold	5-fold	3	0.40	0.37
Pt(432)	120° corner	A-side	4-fold	4	0.99	0.84
Pt(432)	120° corner	4-fold	B-side	4	0.40	0.38
Pt(432)	120° corner	B-side	4-fold	4	0.90	0.76
Pt(432)	120° corner	4-fold	A-side	4	0.49	0.44

[a] Ref. 10

[b] Ref. 8

[c] This compares to an FIM value (see Ref. 20) of 0.84±0.10 eV at B-steps on Pt(331).

Table 3:

path	LDA	GGA	semi-empirical	Exp't
along A-step	0.84	0.71	~0.45[a]	
along B-step	0.90	0.77	~0.40[a]	0.84[c]
corner-to-A	0.49	0.44	0.21,[b] 0.23-0.25[a]	
corner-to-B	0.40	0.38	0.17,[b] 0.18-0.20[a]	
Pt(311)	0.77	0.64		0.60,[d] 0.69[c]

[a]Ref. 2

[b]Ref. 15

[c]Ref. 20

[d]Ref. 21

Table 4:

Step type	Adatom site	shortest adatom bonds
A	5-fold	2.58(b),2.58(b),2.64(e),2.64(e),2.71(t)
A	barrier	2.47(b),2.64(e),2.73(t),2.73(t)
B	5-fold	2.56(b),2.64(e),2.64(e),2.66(t),2.66(t)
B	barrier	2.47(e),2.49(t),2.76(b),2.76(b)
no step	3-fold (fcc)	2.52(t),2.52(t),2.52(t)
no step	bridge	2.47(t),2.47(t)

Table 5:

vicinal	barrier	shortest adatom bonds
Pt(221)	along B-step bottom	2.47(e),2.49(t),2.76(b),2.76(b)
Pt(874)	B-edge to corner	2.47(e),2.50(t),2.71(b),2.79(b)
Pt(322)	along A-step bottom	2.47(b),2.64(e),2.73(t),2.73(t)
Pt(854)	A-edge to corner	2.47(b),2.61(e),2.66(t),2.92(t)

Fig. 1a
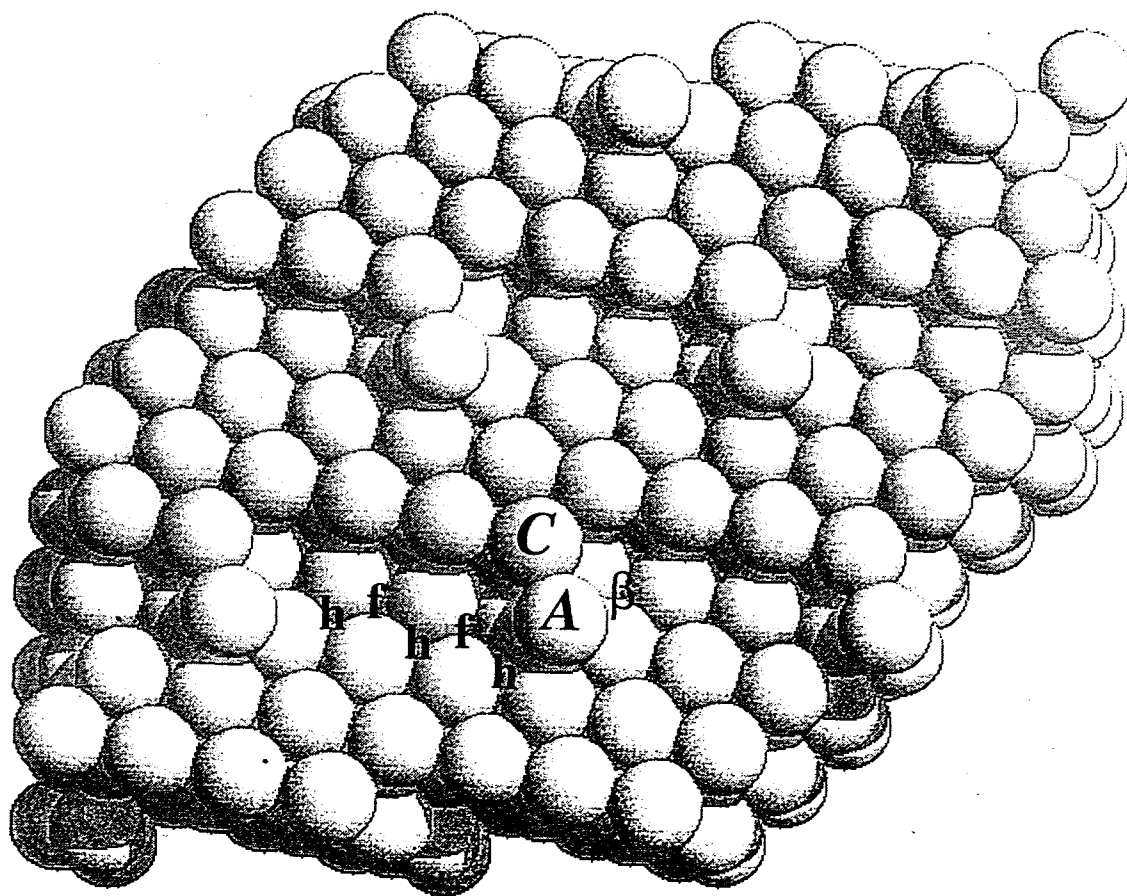
Fig. 1b
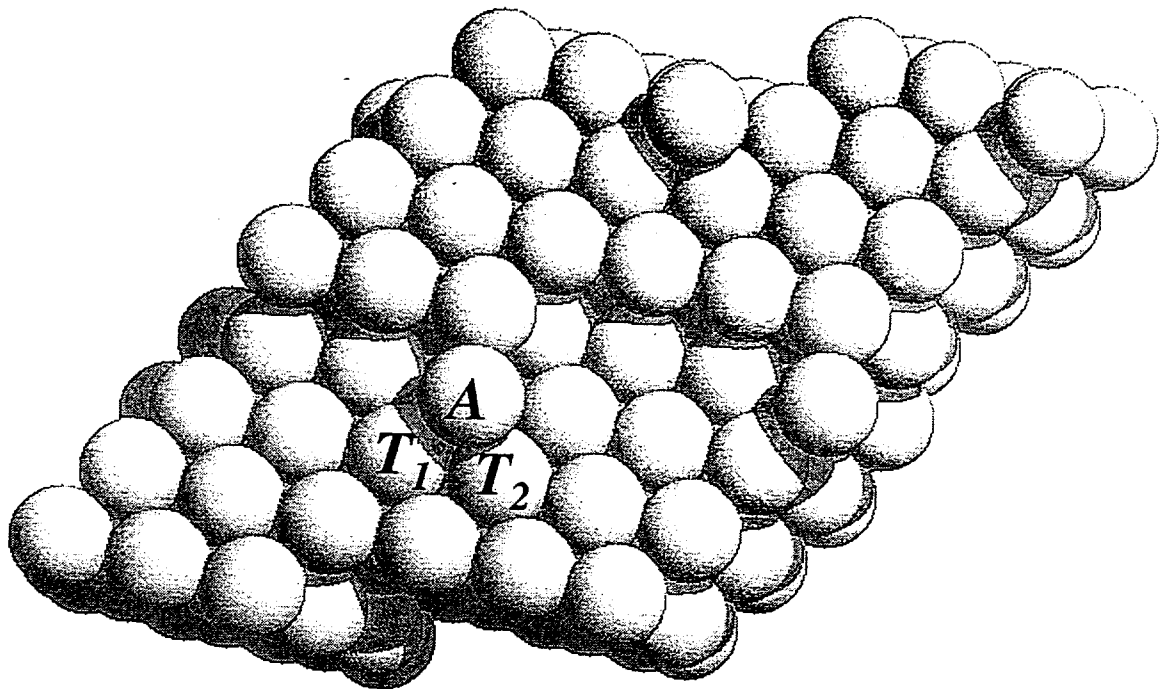
Fig. 2a
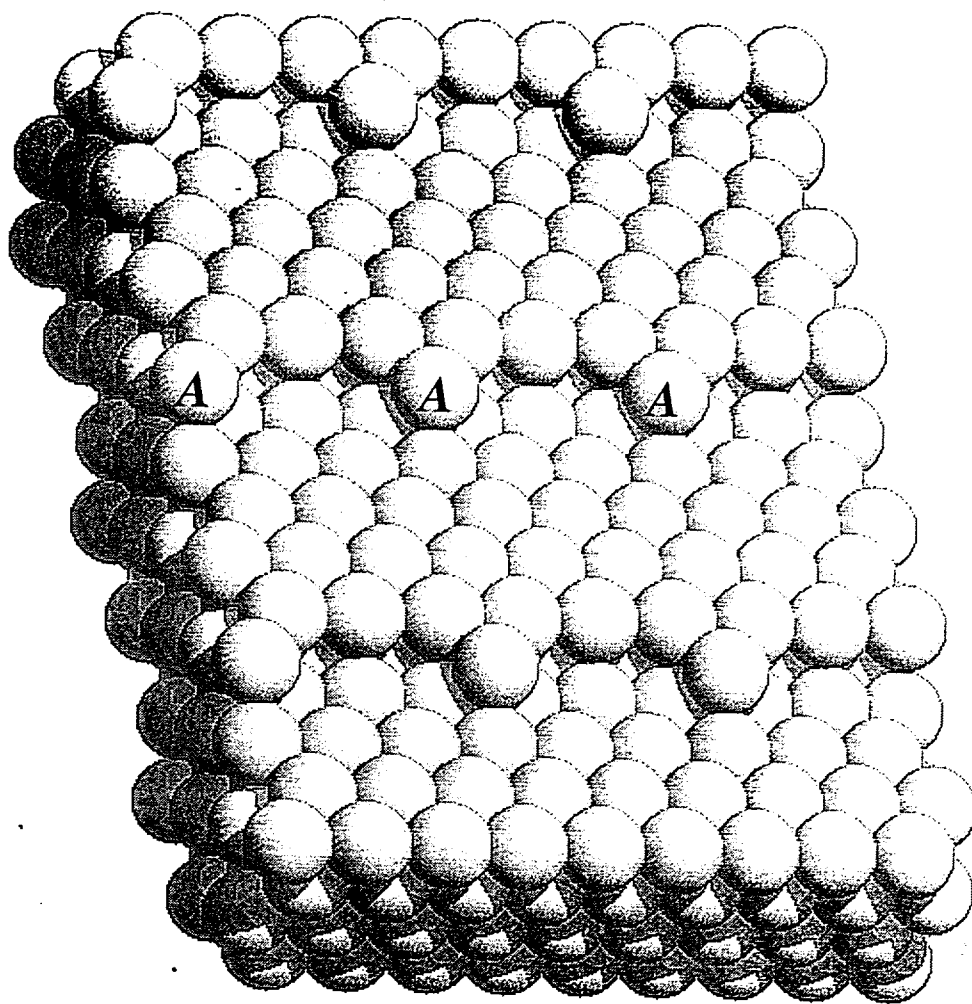
Fig. 2c
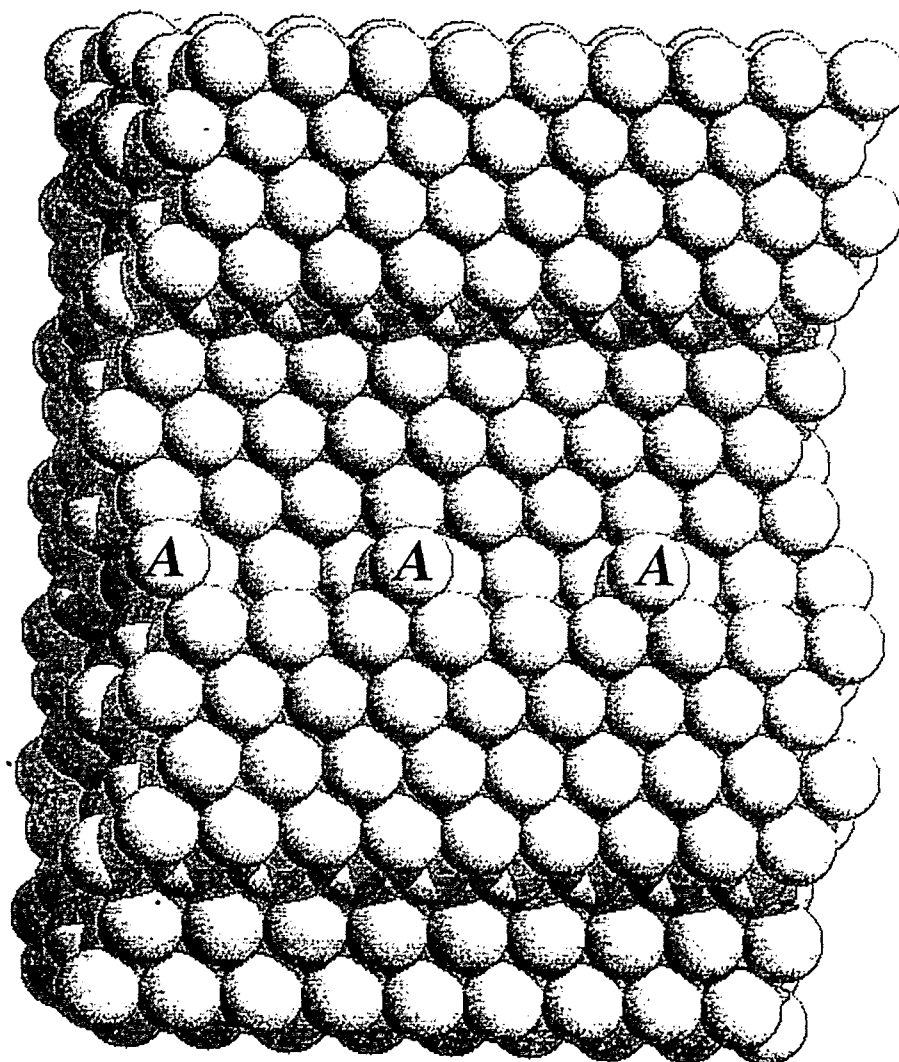
Fig. 3a
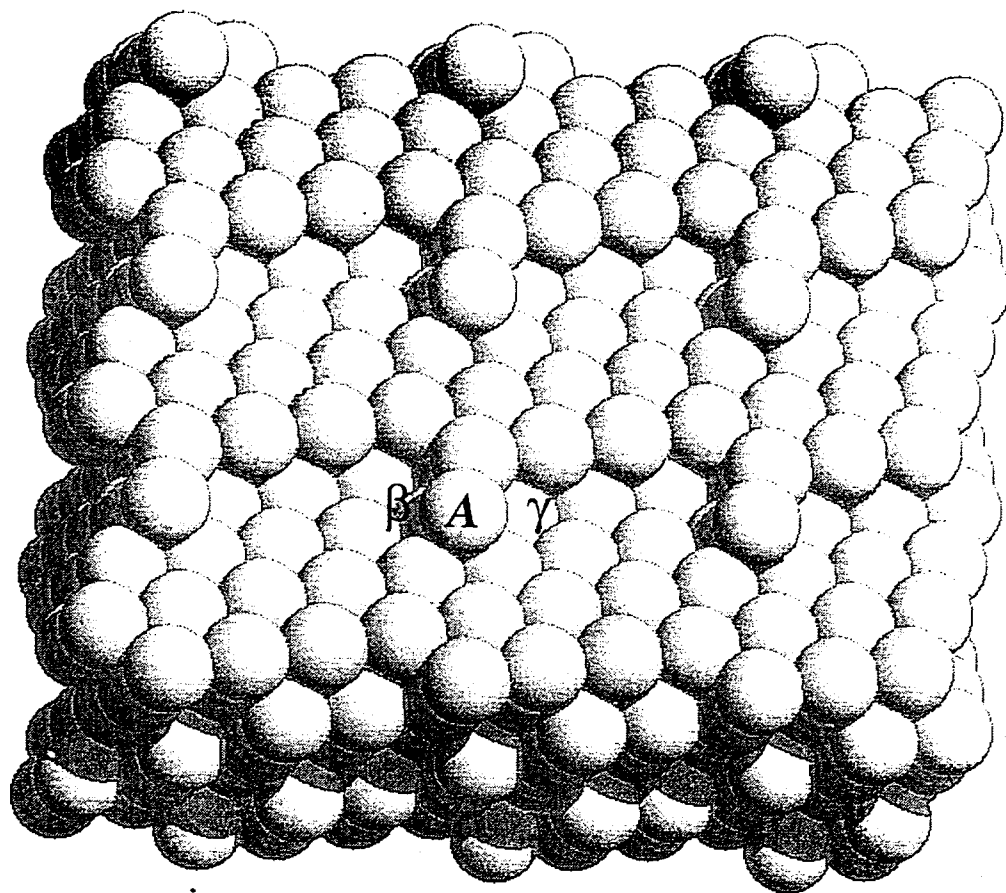
Fig. 3b
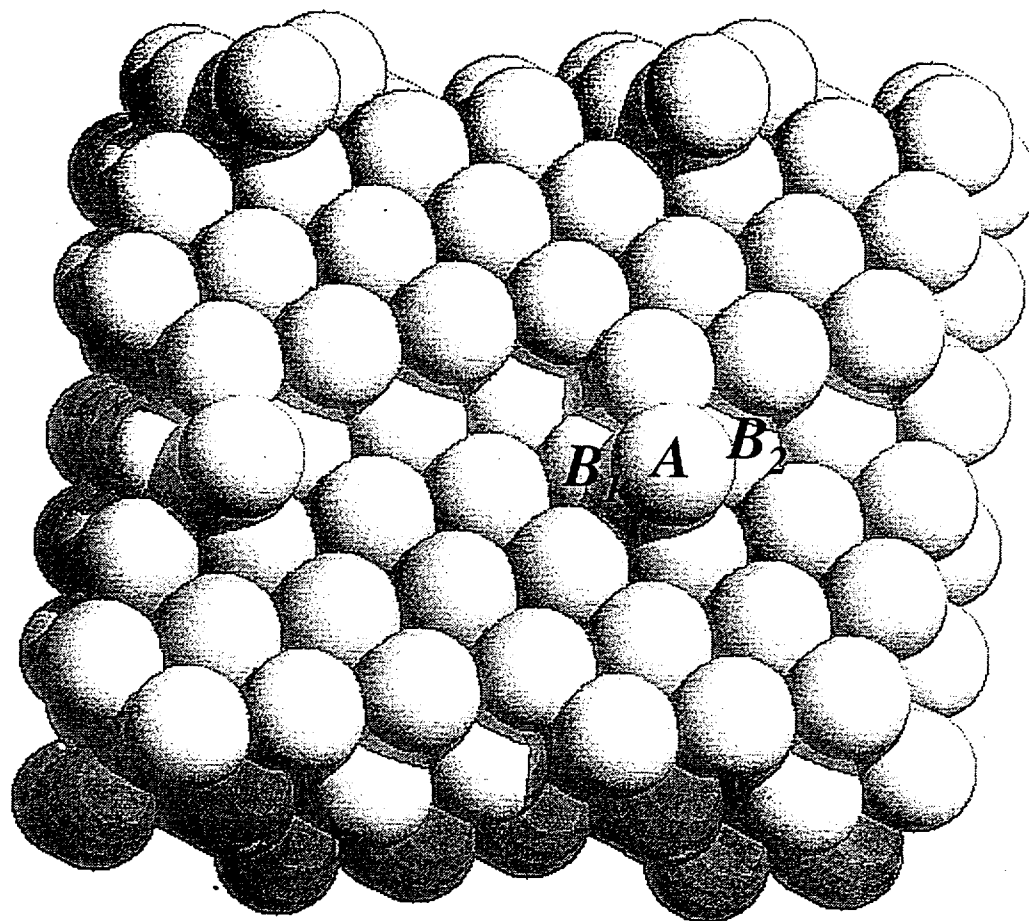
Fig. 4a
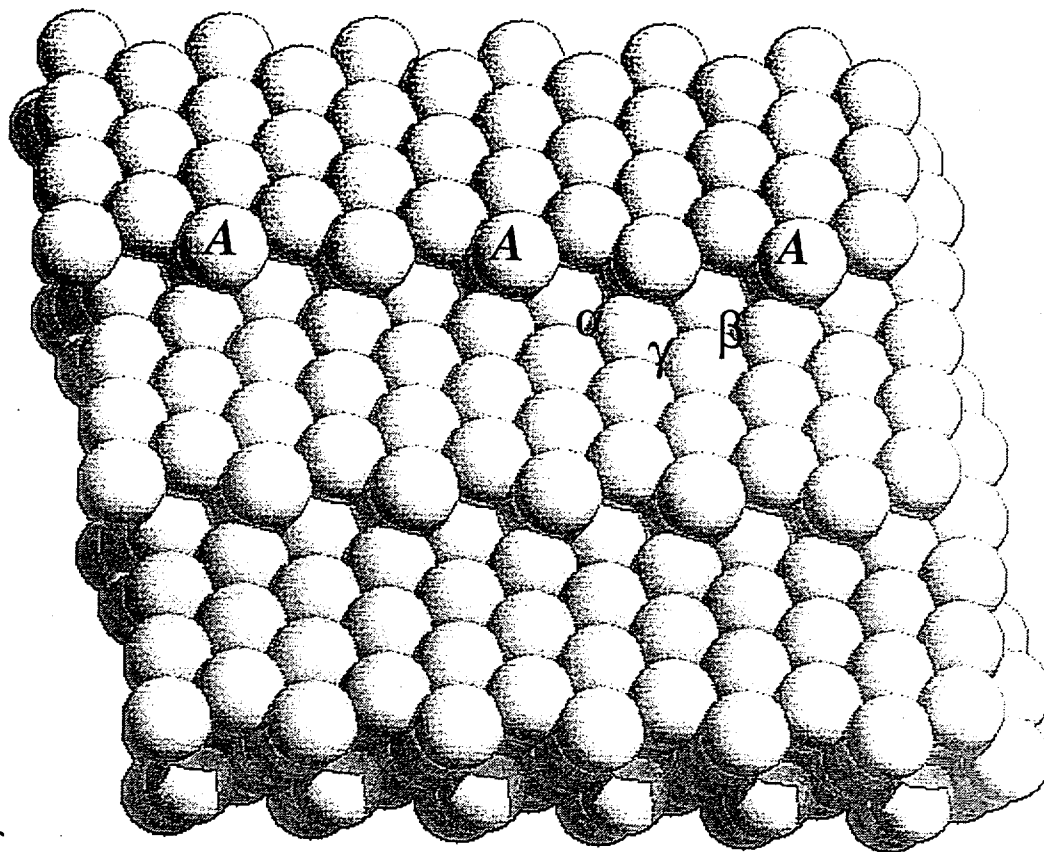
Fig. 4b

Fig. 4c

Fig. 5

Fig. 6a

Fig. 6b